Freeze-thaw Assessment of Plants Based on Envelope Analysis of Stem Volume Water Content Sequence

Hao Tian
Beijing Technology and Business University
Chao Gao (gaochao9158@sina.com)
Beijing Technology and Business University https://orcid.org/0000-0002-0873-2826
Xin Zhang
Beijing Technology and Business University
Hongbing Xiao
Beijing Technology and Business University
Chongchong Yu
Beijing Technology and Business University

Research Article

Keywords: standing wave ratio, stem volume water content, stem volume ice content, stem freeze-thaw rate of ice, envelope analysis, freeze-thaw model

Posted Date: December 3rd, 2021

DOI: https://doi.org/10.21203/rs.3.rs-1114090/v1

Abstract

Background: Frost stress is an abiotic stressor for plant growth that impacts the health and the regional distribution of plants. The freeze-thaw characteristics of plants during the overwintering period help to understand relevant issues in plant physiology, including plant cold resistance and cold acclimation. Therefore, we aimed to develop a non-invasive instrument and method for accurate in situ detection of changes in stem freeze-thaw characteristics during the overwintering period.

Results: A sensor was designed based on standing wave ratio method (SWR) to measure stem volume water content (StVWC). We were able to measure stem volume ice content (StVIC) and stem freeze-thaw rate of ice (StFTRI) during the overwintering period. The resolution of the StVWC sensor is less than 0.05 %, the mean absolute error and root mean square error are less than 1 %, and the dynamic response time is 0.296 s. The peak point of the daily change rate of the lower envelope of the StVWC sequence occurs when the plant enters and exits the overwintering period. The peak point can be used to determine the moment of freeze-thaw occurrence, whereas the time point corresponding to the moment of freeze-thaw coincides with the rapid transition between high and low ambient temperatures. In the field, the StVIC and StFTRI of *Juniperus virginiana* L., *Lagerstroemia indica* L*.* and *Populus alba* L. gradually increased at the beginning, fluctuated steadily during, and then gradually decreased by the end of the overwintering period. The StVIC and StFTRI also showed significant variability due to differences among the tree species and latitude.

Conclusions: The StVWC sensor has good resolution, accuracy, stability, and sensitivity. The envelope changes of the StVWC sequence and the correspondence between the freeze-thaw moment and the ambient temperature indicate that the determination of the freeze-thaw moment based on the peak point of the daily change rate of the lower envelope is reliable. The results show that the sensor is able to monitor changes in the freeze-thaw characteristics of plants and effectively characterize freeze-thaw differences and cold resistance of different tree species. Furthermore, this is a cost-effective tool for monitoring freeze-thaw conditions during the overwintering period.

Background

Frost is an atypical biological stress to woody plants in temperate and cold climates. It affects plant growth and distribution [1,2] by affecting mechanisms related to the diffusion of ice crystals, changes in cell membrane fluidity, and osmoregulation of ion migration. However, freezing and thawing of plants is a process of mutual transformation of liquid water and solid ice. During the overwintering period, when the plant temperature is lower than the freezing point, the water in liquid state is frozen and turned into solid ice crystals in plants. When the plant temperature is higher than the freezing point, these solid ice crystals melt again and turn into liquid water in the tissues [3]. Plants undergo a cyclic process of alternating liquid water and solid ice in their bodies. However, this freeze-thaw cycle can damage tissues or organs of the tree and even lead to death [4–6].

The freeze-thaw characterization of plants can be assessed by their morphology, the half-lethal temperature (LT50) and the subcooling point [7,8]. The improvement of technology and instrumentation allowed the analysis of several biochemical metabolic indicators (e.g., enzyme activity, soluble proteins, respiration, etc.) in plant tissues. These indicators can also provide a more accurate assessment of the current state of the plant, providing a reference for the analysis of freeze-thaw characteristics of the plant [9]. However, these methods are not feasible on a large scale because of expensive equipment and high requirements for the operator. In recent years, with the development of image analysis technology, some scholars have detected the freezing and thawing of plants with nuclear magnetic resonance (NMR) by scanning the frozen and thawed parts of plants [10,11]. Some researchers have also used infrared imaging equipment to observe the temperature changes on the plant surface during freezing and thawing [12]. However, these devices are expensive and have strict limitations in their use, making it difficult to apply them in a practical context of agriculture and forestry.

Online nondestructive monitoring of freeze-thaw change information in plants in a practical context, has been proposed by Raschi et al. [13], with the use of ultrasound to detect freeze-thaw changes in plants and study the relationship between freeze related gas bursts in plants and ultrasound emission. Later, Charrier et al. used ultrasonic emission analysis to investigate ice nucleation and propagation processes in plant xylem, and the freezing dynamics of plants during freeze-thaw. They found that cavitation near the ice surface after freezing was closely related to ultrasonic emission [14]. Sparks et al. used a time domain reflectometry (TDR) sensor to detect the ice content in winter stems of *Pinus contorta* and found values between 0% and 75% [4,15]. TDR and ultrasound emission methods have the advantage of being nondestructive or minimally destructive, but high cost is a drawback that limits their use. Therefore, this study proposes a freeze-thaw detection method for plants based on the envelope analysis of StVWC sequence. The main subjects of this paper are: (1) the development of a low-cost StVWC sensor, (2) the establishment of a freeze-thaw description model based on envelope analysis of StVWC sequence, and (3) the monitoring of freeze-thaw changes and performing freeze-thaw decoding during the overwintering period of plants.

Material And Methods

StVWC measurement principle and sensor

The principle of measuring the StVWC based on the standing wave ratio (SWR) and the dielectric properties of plant tissues is shown in Fig. 8. When 100 MHz electromagnetic wave generated by the signal source is transmitted along a coaxial transmission line, the impedance of the ring probe installed at the stem does not match the impedance of the transmission line. The electromagnetic wave will be reflected when transmitted to the probe; and then the incident and the reflected waves on the transmission line will be superimposed to form a standing wave [28,29]. The peak and trough values of the standing wave signal are measured at both ends of the transmission line and the difference between the peak and trough values is calculated (Eq. 1).

$$\Delta U = \beta\left(U_a - U_b\right) = 2A\beta\frac{Z_l - Z_0}{Z_l + Z_0}$$

1

where β is the amplification of the amplifier; A is the amplitude of the electromagnetic wave output from the signal source; the coaxial transmission line impedance (Z_0) is 50 Ω; β and A are deterministic values, so that the voltage difference ΔU across the transmission line is only linearly related to the probe impedance (Z_l). Thus, a change in the StVWC will cause a change in the stem dielectric constant, which will lead to a subsequent change in the impedance at the probe. The StVWC can be calculated by establishing the relationship equation between ΔU and the StVWC (Eq. 2), with a and b as calibration coefficients.

$$StVWC = a * \Delta U + b$$

2

The StVWC sensor designed in this study is shown in Fig. 9. It consists of two ring electrodes: American Society of Testing Materials (ASTM) 304 stainless steel with 12.6 mm of width and 0.65 mm of thickness with the adjustment knob on the electrode. The diameter of the ring electrode can be adjusted to different trunk diameters within the range of 30–80 mm (Fig. 9a). The hardware system is shown in Fig. 9b; it converts stem water information into electrical signals and the outputs are sent to the data processing unit. Then the temperature measurement module (DS18B20, Risym, China, range: -45°C–85°C, accuracy: ±0.5°C) synchronizes the acquired ambient temperature information. Subsequently, the data processing unit calculates the stem freeze-thaw information (StVIC, StFTRI) and transmits the data to the database via general packet radio service (GPRS) unit for real-time measurements. The StVWC sensor enclosure is made of white resin (DSM-IMAGE8000, Royal DSM, Netherlands), as shown in Fig. 9c, which has a dielectric constant (< 4) that does not affect the measuring performance of the sensor. The screw on the ring electrode has to pass through the hole and then the electrode interface can be connected. When the three main components are connected together, the assembled stem freeze-thaw sensor is ready as shown in Fig. 9d.

The relationship between the output voltage values of the StVWC sensor circuit and the true values of StVWC was obtained with calibration relationship coefficients to ensure the accuracy of the measurements. Fresh stem segments of *Juniperus virginiana* L., *Lagerstroemia indica* L., and *Populus alba* L. were selected as calibration samples. The stem segments were all 6 cm in length and the volume of the samples was measured by the overflow method after soaking in water. Afterwards, the sensor was mounted on the stem and placed in a drying oven set to 45°C (DHG-9037A, HASUC, China, range: 10□200°C, accuracy: ±1°C). The mass of the stems was weighed every 6 h and the corresponding voltage values were recorded until the stems were completely dry. Finally, the true values of StVWC were calculated with the variation in stem volume and stem mass; and a linear fit was applied to the voltage values and the true values of StVWC to obtain the calibration coefficients.

Concomitantly, the response characteristics of the sensor to the time-varying input quantity was measured with the sensor probe placed in the air. When the sensor output stabilized, a 500 ml beaker was filled with water, and the sensor probe was quickly immersed into the water. This is the input signal, the time of the input is a first-order step signal. The dynamic characteristics were obtained by measuring the variation of the output voltage signal of the sensor with the input using an oscilloscope (TBS1052C, TEKTRONIX, American).

Freeze-thaw Model Of Plant Stem

Many trees or shrubs enter the overwintering period with essentially zero transpiration and minimal root water uptake [30]; therefore, StVWC can be a stable value during the overwintering period (Sun et al., 2019). In addition, the dielectric constant of water is 81 (25°C) and the dielectric constant of ice is approximately 3 (similar to the dielectric constant of dry matter in the stem of a plant) [20]. That means when the water in the stem is converted to ice, the StVIC can be calculated by the reduction in the StVWC before and after freezing and thawing. The key to the calculation is finding the moment when the freezing and thawing of the stem occurs [15,17].

Envelope analysis is a common method for the time series signal processing [31]. This study proposes and establishes a stem freeze-thaw detection method based on the envelope analysis of the StVWC sequence, to address the characteristics of its regular fluctuation over time during the overwintering period. The schematic diagram for calculating the StVIC is shown in Fig. 10. StVWC fluctuated in time, and the peak values (maximum and minimum) in each cycle of StVWC were connected to obtain the upper and lower curves with time, which are the upper envelope (δ^a) and lower envelope (δ^b). As the water in the stem is converted to ice during the overwintering period, the StVWC and the lower envelope (δ^b) decrease significantly before leveling off, and the daily change rate of δ^b is expressed by $\Delta\delta^b$(Eq. 3),

$$\Delta\delta^b = {\delta^b}_{t2} - {\delta^b}_{t1}$$

3

where ${\delta^b}_{t2}$ and ${\delta^b}_{t1}$ are the δ^b corresponding to the adjacent moments $t2$ and $t1$ respectively. When the peak point of $\Delta\delta^b$ appears, the stem is considered to be in the freeze-thaw state. Then the moment $t1$ and the corresponding value of the upper envelope ${\delta^a}_{t1}$ are recorded; and the StVIC after moment $t1$ is calculated using Eq. 4,

$$StVIC_{tx} = \frac{{V^{ice}}_{tx}}{V} \times 100\% = \frac{({\delta^a}_{t1} - {\delta^w}_{tx}) \times \rho_w}{\rho_{ice}} \times 100\%$$

4

where, $StVIC_{tx}$ is the volume of ice in the stem at moment tx; ${V^{ice}}_{tx}$ is the volume of ice in the stem at moment tx; V is the volume of the stem; ${\delta^w}_{tx}$ is the volume of water in the stem at moment tx during freeze-thaw; ρ_w is the density of water; and ρ_{ice} is the density of ice.

Excessive freezing of plants during freeze-thaw will result in massive cell death, that causes irreversible damage to the plant [4,6]. Therefore, StFTRI is another important indicator of the freeze-thaw characteristics of plants, calculated by Eq. 5,

$$StFTRI_{tx} = \frac{\left|StVIC_{tx'} - StVIC_{tx}\right|}{\left|tx' - tx\right|}$$

5

where $StFTRI_{tx}$ is the freeze-thaw rate of ice in the stem at moment tx; and $StVIC_{tx'}$ is the volume of ice in the stem corresponding to tx' at an adjacent moment after tx.

Plant Materials

The plant materials were *Juniperus virginiana* L., *Lagerstroemia indica* L. and *Populus alba* L.. *Juniperus virginiana* L. was 5 years old with a height of 2.65 m and a stem diameter of 5.98 cm (Fig. 11a). *Lagerstroemia indica* L. was 3 years old with a height of 2.7 m and a stem diameter of 3.2 cm (Fig. 11b). *Populus alba* L. was 8 years old with a height of 7.5 m and a stem diameter of 8.2 cm (Fig. 11c). Stems were cut from these trees for sensor calibration and testing during non-freeze–thaw periods. The StVWC sensor was installed at 1 m of height above the ground of all trees.

Field Freeze-thaw Experiments

The freeze-thaw experiments were conducted outdoors, and the parameters of the overwintering plant material were recorded by sensors for measuring StVWC, StVIC, StFTRI, and daily average ambient temperature (T-Mean). The measurement dates were from 2018.10.15 to 2019.3.20 for *Juniperus virginiana* L.; from 2018.10.22 to 2019.3.21 for *Lagerstroemia indica* L.; and from 2018.10.1 to 2019.4.19 for *Populus alba* L.. *Juniperus virginiana* L. is located in Hohhot, Inner Mongolia, China (111°50′28″E, 40°32′34″N), which has a mid-temperate continental climate, and a regional average temperature of 24.0°C in July (hottest) and -10.0°C in January (coldest). *Lagerstroemia indica* L. is located at the Bajia Nurseries in Beijing, China (116°21′14″E, 40°0′55″N), the area has a warm temperate semi-humid semi-arid monsoon climate, and the average temperature in the region is 26.0°C in July (hottest) and -5.0°C in January (coldest). *Populus alba* L. is located in Moule Mountain Forestry, Harbin City, Heilongjiang Province, China (127°34′48″E, 45°16′13″N), the area has a mid-temperate monsoon climate with long winters and short summers; the average temperature in the area is 23.0°C in July (hottest) and -19.0°C in January (coldest), with high inter-month variations in temperature, generally around 8 to 10°C.

Results

Calibration and dynamic response characteristics

The relationship between the true values of the StVWC and the output voltage of StVWC detected by the sensor circuit is shown in Fig. 1. The fitted equation was obtained by linear fitting (Table 1). The fitted coefficients of determination (R^2) of the linear fits were 0.9845, 0.9803, and 0.9892 for each tree species. Values a and b of the fitted equations were used as calibration coefficients to the corresponding tree. The curve of the output dynamics captured by the oscilloscope is shown in Fig. 2 with the dynamic response time being 296 ms.

Table 1 Fitting equation of the true values of StVWC and the output voltage of StVWC sensor circuit (*U)*.

Tree species	Fitting equation	R^2	a	b
Juniperus virginiana L.		0.9845	31.28	-6.13
Lagerstroemia indica L.		0.9803	52.27	-30.97
Populus alba L.		0.9892	49.11	-12.63

Envelope characteristics of StVWC sequence with freeze-thaw moments

The StVWC of *Juniperus virginiana* L., *Lagerstroemia indica* L., and *Populus alba* L. during the overwintering period was analyzed, and the lower envelope of the StVWC ( ) was calculated, as shown in Fig. 3., where fluctuates at a high level at first, then with the onset of winter, decreases rapidly. After entering the overwintering period, stays at a lower level. When spring comes, the plant starts to recover, and the lope rises rapidly again. After the overwintering period, continues to fluctuate at a higher level. The accurate moment when plants enter and leave the freeze-thaw process is determined by the daily change rate of the lower envelope ( ), which is shown in Fig. 3.

As the phases of rapidly decrease and increase, two peaks appear in the daily change rate of the curve. The peak point A (A^1, A^2 and A^3) corresponds to the rapidly decreasing phase or the freezing point of the plant, whereas the peak point B (B^1, B^2 and B^3) corresponds to the rapidly increasing phase or the melting point of the plant. The moment corresponding to point A (A^1, A^2 and A^3) and point B (B^1, B^2 and B^3) is the moment when the plant freezes and thaws. After determining the moment of freezing and thawing, the stem volume ice content (StVIC) is calculated according to equation (4). The freezing point moments of *Juniperus virginiana* L., *Lagerstroemia indica* L. and *Populus alba* L. in Fig. 3 are A^1 (2018/11/14), A^2 (2018/11/15), and A^3 (2018/11/14), respectively; and the melting point moments are B^1 (2019/3/2), B^2 (2019/3/9), and B^3 (2019/3/3), respectively.

Temperature variation of stem freeze-thaw moments

The daily average temperature (T-Mean) of the plant growth environment was also recorded (Fig. 4). T-Mean fluctuations of *Juniperus virginiana* L., *Lagerstroemia indica* L., and *Populus alba* L. ranged from -4.0℃-1.0℃, -6.5℃0.5℃, -7.0℃4.0℃ when the plants were at freezing points A^1, A^2, and A^3, respectively. T-Mean decreased during the overwintering period and the water in the plant reached the zero temperature boundary of liquid-solid conversion. This resulted in a rapid decrease of water and increase

of ice in the plant, causing to fall and to increase instantaneously creating a peak. Thereafter, fluctuated in a smaller range along with the T-Mean fluctuations at low temperatures.

The plants went through the overwintering period and entered the spring budding period. During this period T-Mean fluctuations of *Juniperus virginiana* L., *Lagerstroemia indica* L., and *Populus alba* L. ranged from -1.0°C□0.5°C, -7.0°C□1.0°C, -3.5°C□0.5°C,for melting points B^1, B^2, and B^3, respectively. Once again, as the water in the plant reaches the zero temperature boundary of solid-liquid transition, the ice in the plant begins to melt, resulting in a rapid increase of water content in the plant, further causing a rapid rise in and in creating a peak.

Changes of StVIC during the overwintering period

The changes in the StVIC of *Juniperus virginiana* L., *Lagerstroemia indica* L., and *Populus alba* L. during the overwintering period are shown in Fig. 5. Before the overwintering period, the temperature is high, the plant does not freeze and thaw, and the StVIC is zero. As winter begins, the temperature decreases, the liquid water in the plant is transformed into ice, and the StVIC gradually rises. In the late winter, the temperature is low, and the StVIC further increases and fluctuates within a certain range. When spring starts, the temperature increases, the StVIC starts to decrease, the ice melts into liquid water, and the StVIC gradually decreases until the overwintering period is over.

The fluctuations in StVIC of *Juniperus virginiana* L., *Lagerstroemia indica* L., and *Populus alba* L. during the overwintering period were significantly different. The box plot of StVIC changes are shown in Fig. 6. The size of the boxes describes the magnitude of data volatility, showing that *Juniperus virginiana* L. is the least volatile and *Populus alba* L. is the most volatile.

Changes of StFTRI during the overwintering period

The stem freeze-thaw rate of ice (StFTRI) is closely related to the freeze-thaw process in the plant. When plants go through the overwintering period, the freeze-thaw process is so fast that it causes massive cell death, resulting in irreversible damage to the plant. The changes in StFTRI of *Juniperus virginiana* L., *Lagerstroemia indica* L., and *Populus alba* L. during the overwintering period are shown in Fig. 7. Table 2 shows the results of statistical analysis of the StFTRI volatility.

A little fluctuation of the StFTRI of *Juniperus virginiana* L. can be observed, with a standard deviation of 0.00405 cm^3/cm^3 • min; whereas the StFTRI of *Lagerstroemia indica* L*.* and *Populus alba* L. showed more fluctuation, with standard deviations of 0.02256 cm^3/cm^3 • min and 0.01567 cm^3/cm^3 • min, respectively. In particular, there was a significant large fluctuation throughout the overwintering period for *Lagerstroemia indica* L.; however, *Populus alba* L. only fluctuated significantly in the early overwintering period, with a maximum value of 1.36122 cm^3/cm^3 • min. Moreover, the fluctuation and the value of StFTRI were smaller for *Populus alba* L. when compared to those of *Lagerstroemia indica* L*.*

Table 2 Statistical analyses of StFTRI volatility.

Results of statistical analysis	*Juniperus virginiana* L.	*Lagerstroemia indica* L.	*Populus alba* L.
Mean value (cm^3/cm^3 • min)	0.00294	0.01515	0.0068
Standard deviation (cm^3/cm^3 • min)	0.00405	0.02256	0.01567
Minimum value (cm^3/cm^3 • min)	0	0	0
Maximum value (cm^3/cm^3 • min)	0.04446	0.87662	1.36122

Discussion

Sensor calibration and dynamic response characteristics

Table 1 illustrates a linear relationship between the output voltage of the StVWC sensor circuit and the true values of StVWC, with a coefficient of determination that exceeds 0.98. Combined with the resolution of the analog-to-digital converter (ADC) (0.806 mV), the resolution of the StVWC measured by the sensor can be calculated, which is less than 0.05 %, indicating that the sensor has good resolution and can effectively measure the change in StVWC. The mean absolute error and root mean square error are less than 1%, indicating that the sensor has high accuracy and stability with respect to measurements. Concurrently, the dynamic response time of the sensor is 296 ms (Fig. 2), that meets the actual measurement requirements, indicating that the sensor has good sensitivity.

Determination of the freeze-thaw moment

The conversion of liquid and solid states of water is the basis for calculating the StVIC, which can be obtained by calculating the change in water content in the stem before and after freezing and thawing [4,15,16]. The key to calculate StVIC is to track the freeze-thaw moment [17]. In this study, we propose a method to determine the freeze-thaw moment based on the lower envelope and its daily change rate by analyzing the envelope of the StVWC sequence. The peak point of the daily change rate of the lower envelope (Fig. 3) provides a basis for the determination of the freeze-thaw moment. Previous studies have also shown that freezing of plant tissues occurs when temperature drops below the freezing point, followed by the production of ice crystals in the plant [6,13,18]. The rapid decrease (or increase) of ambient temperature near the solid-liquid transition boundary, indicates the formation (or disappearance) of ice crystals in plant tissues (Fig. 4). The peak of daily change rate of the lower envelope occurs at this time, allowing the determination of the freeze-thaw moment.

Freeze-thaw changes of plants during the overwintering period

The changes in StVIC (Fig. 5) and StFTRI (Fig. 7) of *Juniperus virginiana* L., *Lagerstroemia indica* L., and *Populus alba* L. can be observed during the overwintering period. The StVIC rises continuously from autumn to winter as the plant enters dormancy and vitality decreases. The StVIC

decreases in accordance with the general rule of plant growth process as the plant starts to grow back and vitality increases from winter to spring [19]. Some periodic fluctuations of StVIC were observed during the overwintering period, with a decrease of ice in the stems when the temperature increased during the day; and an increase of ice in the stems when the temperature decreased during the night, confirming the periodic fluctuations of StVIC in previous studies [4,20,21].

Freeze-thaw characteristics of deciduous broadleaf species and evergreen coniferous species

The variation in StVIC of *Lagerstroemia indica* L. (a deciduous broadleaf species) and *Juniperus virginiana* L. (an evergreen coniferous species) can be compared in Fig. 6. The box height of *Lagerstroemia indica* L. was approximately three times the box height of *Juniperus virginiana* L., indicating that the StVIC of *Juniperus virginiana* L. is less volatile during the overwintering period. The StFTRI corresponding to *Juniperus virginiana* L. in Fig. 7 is also small, and the standard deviation of the StFTRI is only 0.00405 (Table 2), indicating that evergreen coniferous species are more capable of regulating themselves during the overwintering period than the deciduous broadleaf species [5,22]. Therefore, *Juniperus virginiana* L. (evergreen coniferous species) is more resistant to cold because of its ability to regulate the ice-water content efficiently and adapt to the overwintering conditions [23,24].

Freeze-thaw characteristics of trees in different latitudes

The higher the latitude, the lower the winter temperature and the colder the overwintering period [25]. The latitude of Beijing is lower than Heilongjiang, therefore, the ambient temperature of Beijing is not as cold as that of Heilongjiang. The StVIC fluctuation of *Lagerstroemia indica* L. in the warm temperate zone of Beijing (Haidian District) ranged from 0 % to 15% (Fig. 5b), and the overwintering StVIC fluctuation of *Populus alba* L. in the middle temperate zone of Heilongjiang (Cap Hill, Harbin) ranged from 0 % to 60% (Fig. 5c). This indicates that *Populus alba* L. was subjected to intense stress by low temperature. However, the fluctuation of StFTRI (Fig. 7c) was less drastic as compared to that of *Populus alba* L. (Fig. 7b) because their stems were thicker and longer due to years of growth. This is supported by the results on the StFTRI volatility (Tab. 2), that show that plants are resistant to cold after cold training. This also proves that latitude and temperature are important factors affecting freezing and thawing of plants; the higher the latitude, the more vulnerable the plants are to freezing and thawing[26,27], which provide a reference for plantation forestry in different latitudinal climatic zones.

Advantages of StVWC sensor

In-depth studies have been conducted in the field of plant water detection. The performance of TDR and frequency domain (FD) principle sensors has been demonstrated in numerous studies. Zhou et al. applied TDR and FD sensors to the stem for freeze-thaw measurements [4,15]; however, these sensors are expensive and invasive. The StVWC sensor designed in this study is inexpensive (approximately $15), capable of dynamic real-time remote monitoring, and easy to use in agriculture and forestry. This sensor

measures the StVIC and StFTRI based on the envelope analysis of the StVWC sequence, providing a technical monitoring method for plant freeze-thaw and forest tree nursery.

Conclusions

In this study, a new, low-cost StVWC sensor was developed based on the dielectric properties of plants and the water-ice conversion relationship during freeze-thaw process of plants. A freeze-thaw analysis model was developed based on the envelope variation of the StVWC sequence to determine the StVIC and StFTRI under field conditions, effectively avoiding damage to plants caused by invasive measurements. Calibration experiments and dynamic response tests showed that the StVWC sensor has good resolution, stability, and sensitivity. Simultaneous measurements on different tree species demonstrated the applicability of the method to a wide range of studies. The freeze-thaw moment was successfully determined by analyzing the lower envelope of StVWC and its daily change rate, and by comparing the ambient temperature with the freeze-thaw moment. The freeze-thaw moment based on the peak point of the daily change rate of the lower envelope was proven to be reliable. The study of freeze-thaw changes in *Juniperus virginiana* L., *Lagerstroemia indica* L., and *Populus alba* L. during the overwintering period, showed that the StVWC sensor can effectively monitor StVIC and StFTRI during freeze-thaw cycles. In addition, the comparison of freeze-thaw values of *Lagerstroemia indica* L. and *Juniperus virginiana* L., as evergreen coniferous species, presented less fluctuation in the StVIC. The StFTRI fluctuation was also small, proving that the sensor could effectively characterize the ability of the plant to resist cold. The freeze-thaw information of *Lagerstroemia indica* L. and *Populus alba* L. showed that *Populus alba* L. at high latitudes had higher StVIC during the overwintering period, indicating that they suffered from intense cold stress. Moreover, the fluctuation of StFTRI of *Populus alba* L. was less drastic than that of *Lagerstroemia indica* L., proving the ability to develop cold resistance after cold training. Therefore, this study provides a theoretical basis for the assessment of freeze-thaw-induced embolism and plant cold resistance, and a cost-effective tool for monitoring freeze-thaw conditions during the overwintering period in the field.

Abbreviations

StVWC	Stem volume water content
SWR	Standing wave ratio
StVIC	Stem volume ice content
StFTRI	Stem freeze-thaw rate of ice
NMR	Nuclear magnetic resonance
TDR	Time domain reflectometry
ADC	Analog-to-digital converters

FD	frequency domain
ASTM	American society of testing materials
GPRS	General packet radio service

Declarations

Acknowledgements

The authors thank Beijing Natural Science Foundation (Grant No. 6214034), Research on Key Techniques of Low Visibility Image Target Detection and Parallel Acceleration under Mine Disaster Conditions (Grant No. 2020-KF-23-06) and the Research Foundation for Youth Scholars of Beijing Technology and Business University for financial support.

Authors' contributions

The work was designed and planned by Hao Tian, and Chao Gao. The experiments were conducted, and data were acquired by Hao Tian and Chao Gao. Data were interpreted by Hao Tian, Chao Gao, Xin Zhang and Hongbing Xiao. The paper was written by Hao Tian, Xin Zhang and Chao Gao and reviewed by Chongchong Yu. All authors read and approved the final manuscript.

Funding

This work is supported by Beijing Natural Science Foundation (Grant No. 6214034), Research on Key Techniques of Low Visibility Image Target Detection and Parallel Acceleration under Mine Disaster Conditions (Grant No. 2020-KF-23-06) and the Research Foundation for Youth Scholars of Beijing Technology and Business University.

Availability of data and materials

The data presented in this study are available on request from the corresponding author.

Competing interests

The authors declare that they have no competing interests.

Ethics approval and consent to participate

Not applicable.

Consent for publication

All authors give consent for the data to be published.

References

1. Sanghera G, H. Wani S, Hussain W, B. Singh N. Engineering Cold Stress Tolerance in Crop Plants. Curr Genomics. 2011;12:30–43. https://doi.org/10.2174/138920211794520178.
2. Serman FV, Babelis G, Gallego ME, Lopez E, Sierra E. A frost regime microclimatological study in southern argentina (aelo, province of neuqun). Acta Hortic. 2014;1057:147–53. https://doi.org/10.17660/ActaHortic.2014.1057.17.
3. Havis JR. Water movement in woody stems during freezing. Cryobiology. 1971;8:581–5. https://doi.org/10.1016/0011-2240(71)90012-5.
4. Sparks JP, Campbell GS, Black AR. Water content, hydraulic conductivity, and ice formation in winter stems of Pinus contorta: a TDR case study. Oecologia. 2001;127:468–75. https://doi.org/10.1007/s004420000587.
5. Burke MJ, Gusta LV, Quamme HA, Weiser CJ, Li PH. Freezing and injury in plants. Annu Physiol 1976;27:507–28. https://doi.org/10.1146/annurev.pp.27.060176.00 2451.
6. Wisniewski M, Neuner G, Gusta L V. The use of high-resolution infrared thermography (HRIT) for the study of ice nucleation and ice propagation in plants. J Vis Exp. 2015;2015:1–11. https://doi.org/10.3791/52703.
7. Bai Z, Wuren T, Liu S, Han S, Chen L, McClain D, et al. Intermittent cold exposure results in visceral adipose tissue “browning” in the plateau pika (Ochotona curzoniae). Comp Biochem Physiol -Part A Mol Integr Physiol. 2015;184:171–8. https://doi.org/10.1016/j.cbpa.2015.01.019.
8. Kalushkov P, Nedved O. Cold hardiness of pyrrhocoris apterus (heteroptera: pyrrhocoridae) from central and southern europe. Eur J Entomol. 2013;97:149–53. https://doi.org/10.14411/eje.2000.027.
9. Kurbidaeva AS, Novokreshchenova MG. Genetic control of plant resistance to cold. Russ J Genet. 2011;47:646–61. https://doi.org/10.1134/S1022795411050115.
10. Charrier G, Nolf M, Leitinger G, Charra-Vaskou K, Losso A, Tappeiner U, et al. Monitoring of freezing dynamics in trees: A simple phase shift causes complexity. Plant Physiol. 2017;173:2196–207. https://doi.org/10.1104/pp.16.01815.
11. Hacker J, Neuner G. Ice propagation in plants visualized at the tissue level by infrared differential thermal analysis (IDTA). Tree Physiol. 2007;27:1661–70. https://doi.org/10.1093/treephys/27.12.1661.
12. Devireddy R V., Raha D, Bischof JC. Measurement of water transport during freezing using differential scanning calorimetry. Am Soc Mech Eng Bioeng Div BED. 1996;34:37–41.
13. Raschi A, Mugnozza GS, Surace R, Valentini R, Vazzana C. The use of ultrasound technique to monitor freezing and thawing of water in plants. Agric Ecosyst Environ. 1989;27:411–8. https://doi.org/10.1016/0167-8809(89)90101-1.
14. Charrier G, Pramsohler M, Charra-Vaskou K, Saudreau M, Améglio T, Neuner G, et al. Ultrasonic emissions during ice nucleation and propagation in plant xylem. New Phytol. 2015;207:570–8.

https://doi.org/10.1111/nph.13361.

15. Sun Y, Zhou H, Shan G, Grantz DA, Schulze Lammers P, Xue X, et al. Diurnal and seasonal transitions of water and ice content in apple stems: Field tracking the radial location of the freezing- and thawing-fronts using a noninvasive smart sensor. Agric For Meteorol. Elsevier; 2019;274:75–84. https://doi.org/10.1016/j.agrformet. 2019.04.018.
16. Tian H, Gao C, Zhao Y, Zheng Y, Zhao Y. Design of Freeze-thaw Detection Sensor for Standing Forest Stock Based on Latent Heat. Trans Chinese Soc Agric Mach. 2020;51:223–31.
17. Zhao Y, Tian H, Han Q, Gu J, Zhao Y. Real-time monitoring of water and ice content in plant stem based on latent heat changes. Agric For Meteorol. 2021;307:108475. https://doi.org/10.1016/j.agrformet.2021.108475.
18. Mazur, P. Freezing Injury in Plants. Ann.rev.plant Physiol. 1969;20:419–48.
19. Cobb A, Reade JPH. Herbicides and Plant Physiology. Q Rev Biol. 2010;
20. Wullschleger SD, Meinzer FC, Vertessy RA. A review of whole-plant water use studies in tree. Tree Physiol.1998;18:499–512. https://academic.oup.com/treephys/ article-lookup/doi/10.1093/treephys/18.8-9.499.
21. Irvine J, Grace J. Non-destructive measurement of stem water content by time domain reflectometry using short probes. J Exp Bot. 1997;48:813–8.
22. Tang W, Hu X, Xu W, Wang XJ, Pan HT. Assessing the Cold Resistance of Several Crape Myrtle(Lagerstroemia L.) Species and Cultivars. Acta Agric Boreali-Occidentalis Sin. 2012;21:121–6.
23. Jankowski A, Wyka TP, Żytkowiak R, Nihlgård B, Reich PB, Oleksyn J. Cold adaptation drives variability in needle structure and anatomy in P inus sylvestris L. along a 1,900 km temperate–boreal transect. Kudo G, editor. Funct Ecol. 2017;31:2212–23.
24. Bannister P, Neuner G. Frost Resistance and the Distribution of Conifers. Conifer Cold Hardiness; 2001. p. 3–21. http://doi.org/10.1007/978-94-015-9650-3_1.
25. Wiemann MC, Williamson GB. Geographic variation in wood specific gravity: effects of latitude, temperature, and precipitation. Wood Fiber Sci. 2002;34:96–107.
26. Rapp M, Leclerc MC, Lossaint P. The nitrogen economy in a Pinus pinea L. stand. For Ecol Manage. 1979;2:221–31.
27. Reich PB, Oleksyn J. Global patterns of plant leaf N and P in relation to temperature and latitude. Proc Natl Acad Sci. 2004;101:11001–6. https://doi.org/10.1073/pnas.0403588101.
28. Zhao Y, Wang Y. Analysis of sensitivity of soil moisture measurement based on standing-wave ratio. ransactions Chinese Soc Agric Eng. 2002;2002:5–8.
29. Yang Y, Ji EK, Song HJ, Lee EB, Kim HJ. Methodology: non-invasive monitoring system based on standing wave ratio for detecting water content variations in plants. Plant Methods. 2021;17:1–9. https://doi.org/10.1186/s13007-021-00757-y

30. Allen ST, Kirchner JW, Braun S, Siegwolf RTW, Goldsmith GR. Seasonal origins of soil water used by trees. Hydrol Earth Syst Sci. 2019;23:1199–210. https://hess.copernicus.org/articles/23/1199/2019.
31. Luz, García, Isaac, Álvarez, Manuel, Titos, et al. Automatic Detection of Long Period Events Based on Subband-Envelope Processing. IEEE J Sel Top Appl Earth Obs Remote Sens. 2017; https://doi.org/10.1109/JSTARS.2017.2739690.

Figures

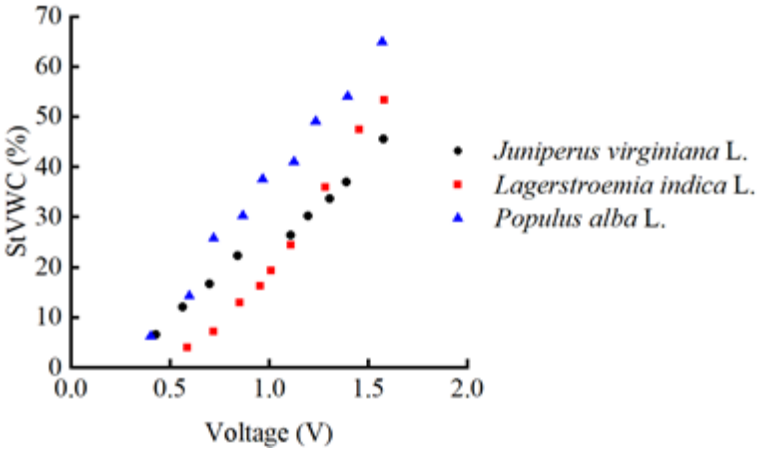

Figure 1

Relationship between the true values of the StVWC and the output voltage of StVWC detected by the sensor circuit.

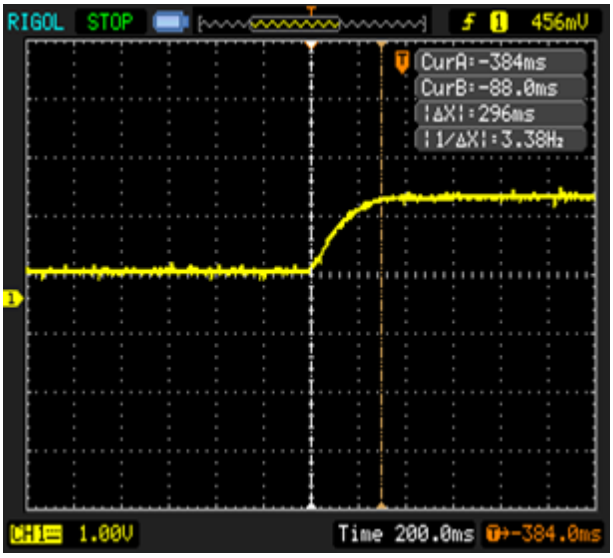

Figure 2

Characteristic curve of the StVWC sensor circuit dynamic response.

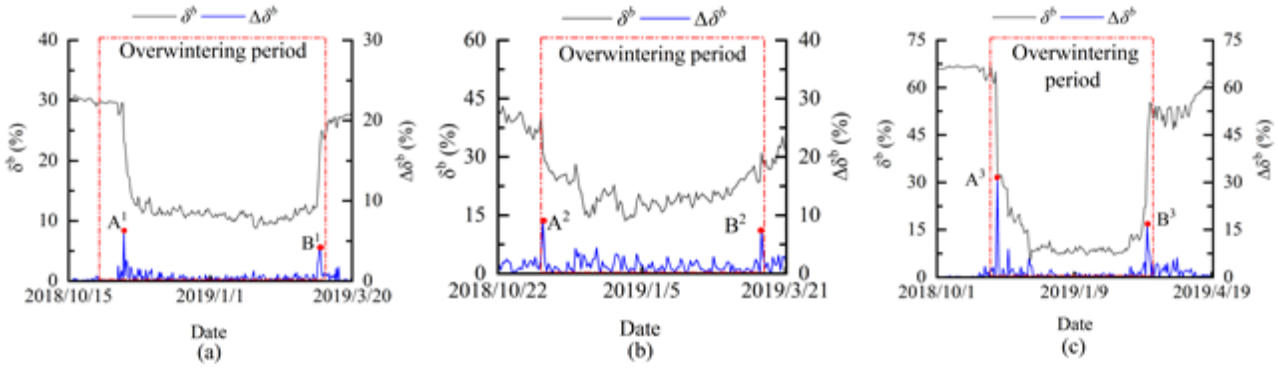

Figure 3

Envelope characteristic of StVWC sequence curves. δ^b: lower envelope of the StVWC. Δδ^b: daily change rate of the lower envelope. (a) Juniperus virginiana L. (b) Lagerstroemia indica L. (c) Populus alba L. Freezing point moments : A1, A2 and A3. Melting point moments : B1, B2, and B3.

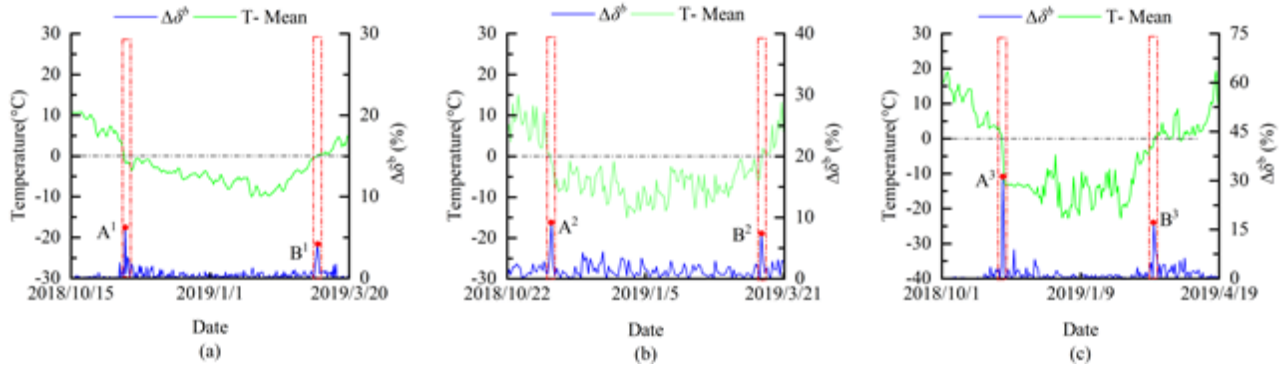

Figure 4

Daily average ambient temperature curve during the overwintering period. Δδ^b: daily change rate of the lower envelope. T-Mean: daily average ambient temperature. (a) Juniperus virginiana L. (b) Lagerstroemia indica L. (c) Populus alba L. Freezing point moments : A1, A2 and A3. Melting point moments : B1, B2, and B3.

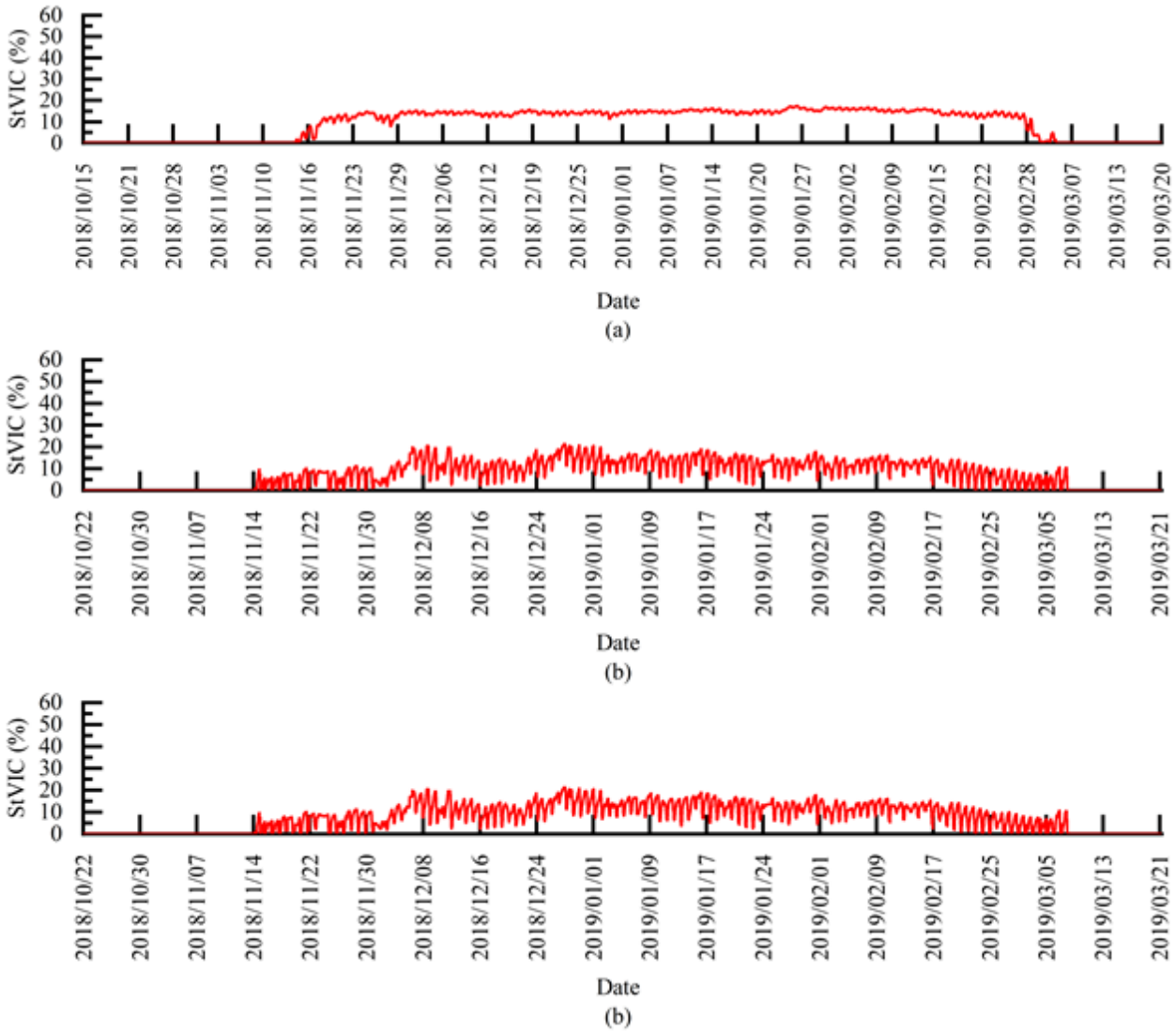

Figure 5

Changes of StVIC during the overwintering period. (a) Juniperus virginiana L. (b) Lagerstroemia indica L. (c) Populus alba L.

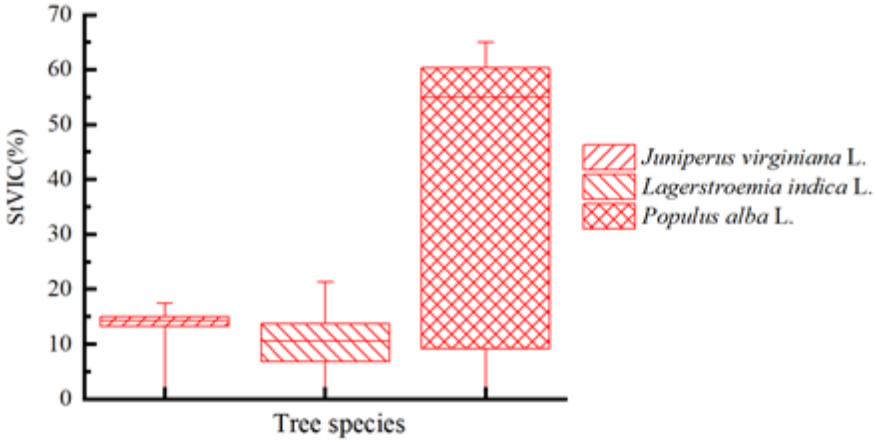

Figure 6

Box plot of the StVIC changes during the overwintering period. (a) Juniperus virginiana L. (b) Lagerstroemia indica L. (c) Populus alba L.

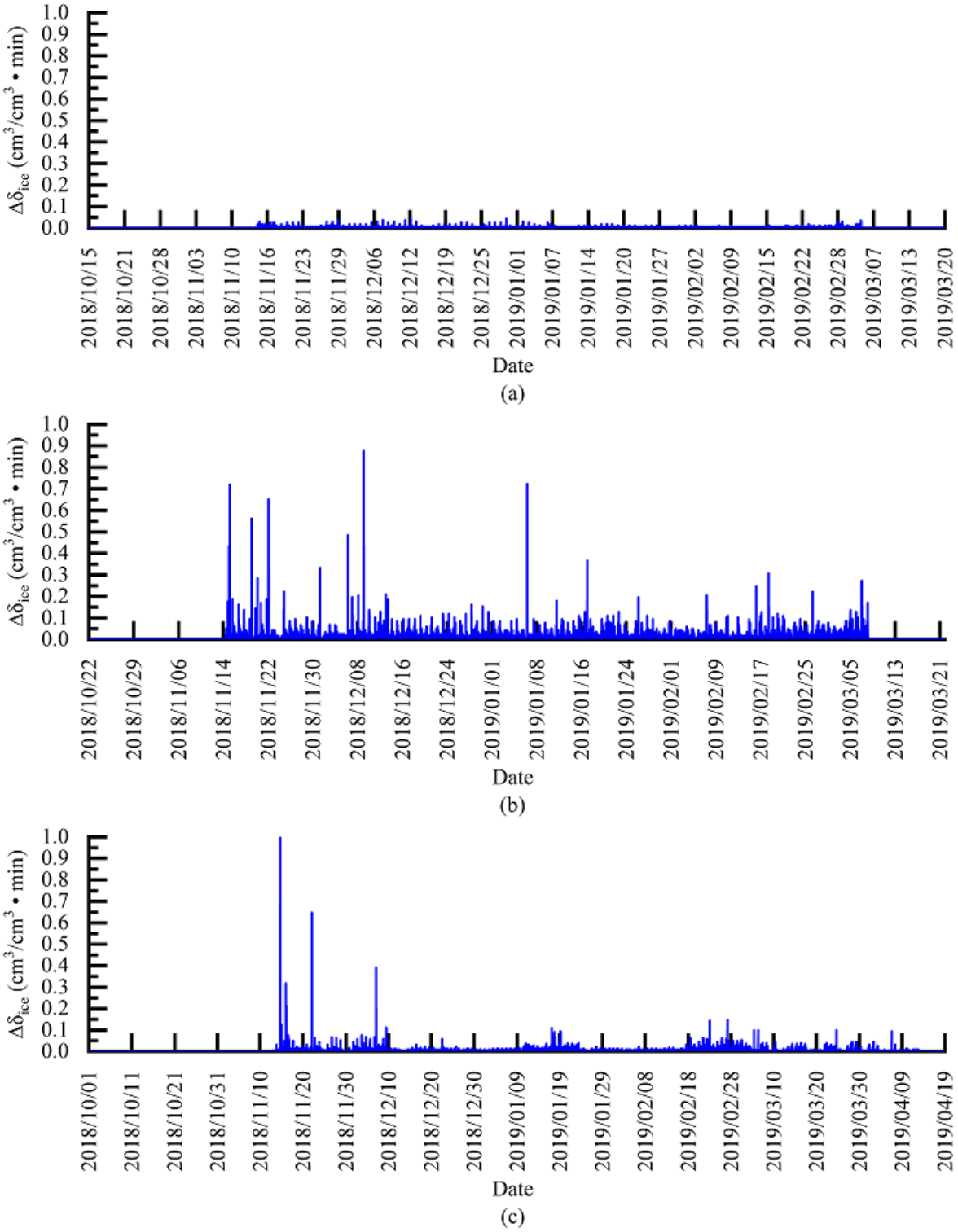

Figure 7

Changes of StFTRI during the overwintering period. (a) Juniperus virginiana L. (b) Lagerstroemia indica L. (c) Populus alba L.

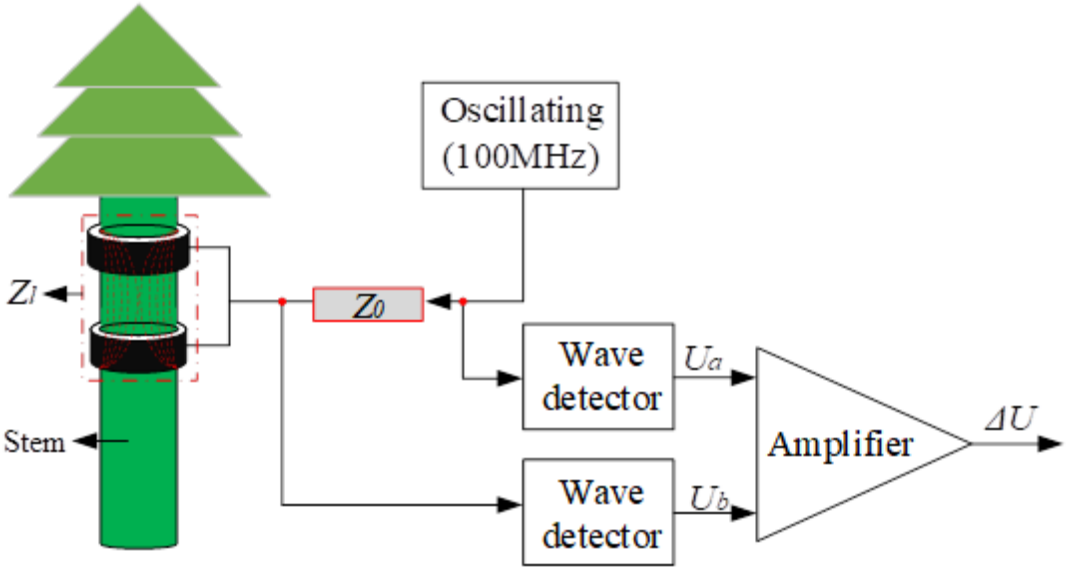

Figure 8

Principle of measurement of stem volume water content. U_a and U_b refer to the outputs of the two wave detecors and the inputs of the amplifier. Z_0: coaxial transmission line impedance. Z_l: probe impedance.

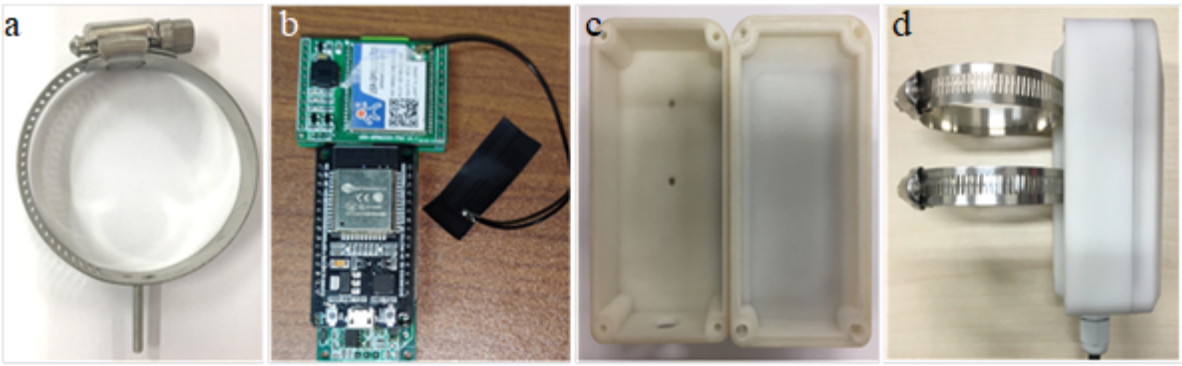

Figure 9

StVWC sensors. (a) Ring electrodes. (b) Hardware system of StVWC sensor. (c) StVWC sensor enclosure. (d) Completed assembly of the sensor.

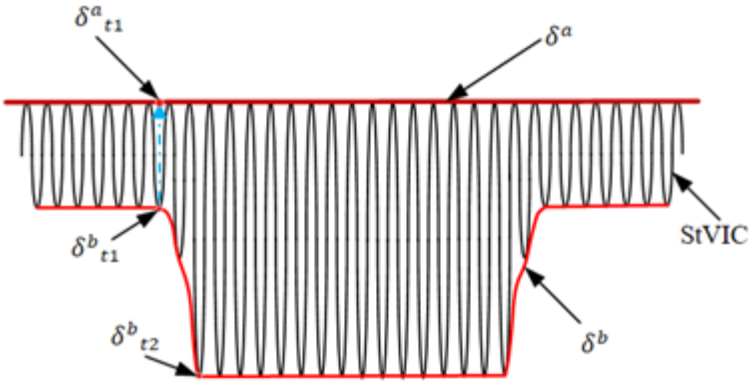

Figure 10

Schematic diagram of the calculation of StVIC based on envelope analysis of StVWC sequence. δ^a and δ^b are the upper envelope and the lower envelope of StVWC, respectively; δ^b_t2 and δ^b_t1 are the δ^b corresponding to the adjacent moments t2 and t1, respectively; and δ^a_t1 is the value of the upper envelope corresponding to the moment t1.

Figure 11

Plant material used for the experiments. (a) Juniperus virginiana L. (b) Lagerstroemia indica L. (c) Populus alba L.